American Mineralogist, Volume 94, pages 1679–1686, 2009

Sideronatrite, $Na_2Fe(SO_4)_2(OH)\cdot 3H_2O$: Crystal structure of the orthorhombic polytype and OD character analysis

FERNANDO SCORDARI* AND GENNARO VENTRUTI

Dipartimento Geomineralogico, Università degli Studi di Bari, Via E. Orabona 4, I-70125 Bari, Italy

ABSTRACT

Sideronatrite, $Na_2Fe(SO_4)_2(OH)\cdot 3H_2O$, is a secondary hydrated sulfate occurring in desert areas as the result of pyrite alteration. It is one of the environmental indicators of soil-water processes operating in specific landscapes, and, as a consequence, an important marker of acid mine drainage pollution. Sideronatrite has been demonstrated from its peculiar diffraction pattern to belong to a family of OD structures formed by equivalent layers.

In this work, a crystal with weak diffuse streaks proved to be suitable for a single-crystal X-ray diffraction study. The crystal structure was solved by direct methods and refined by full matrix least-squares (R = 7.4% and R_W = 8.0%) in the space group $P2_12_12_1$ with a = 7.265(2), b = 20.522(6), c = 7.120(2) Å, V = 1061.5(5) Å^3, and Z = 4, using 798 reflections with $I > 3.0\ \sigma(I)$.

Sideronatrite is characterized by infinite $[Fe^{3+}(SO_4)_2(OH)]^{2-}$ octahedral-tetrahedral chains of the type $[M(TO_4)_2\phi]$ running parallel to the **c** axis. These chains are cross-linked by a columnar system of corner-sharing, Na-distorted octahedra along **c** to form corrugated sheets parallel to the (010) plane. Adjacent sheets are hydrogen-bonded through water molecules coordinated by Na atoms. The present results allow a complete description of the OD character of the structure, with the derivation of the OD groupoid and MDO polytypes.

Finally, chemical and structural relationships are taken into account to explain the possible paragenetic sequence concerning several sulfates associated with sideronatrite.

Keywords: Sideronatrite, structure solution, OD character, polytypism

INTRODUCTION

Sideronatrite is a hydrated sulfate of Na and Fe^{3+} occurring in very arid regions and generally associated with other secondary sulfates (Palache et al. 1951). Sideronatrite was originally described by Raimondi (1878), although bartholomite, previously discovered by Cleve (1870), is likely the same mineral. In the past, it was also confused with urusite (or uruzite, urisite, urizite), a mineral from Tscheleken Island (Russia), reported by Frenzel (1879), who deduced optically the orthorhombic symmetry. Chemical analyses performed by different authors (Frenzel 1879; Van Tassel 1956; Césbron 1964) converge to the ideal formula: $Na_2Fe(SO_4)_2(OH)\cdot 3H_2O$.

This mineral is thought to have been formed as the result of pyrite alteration or as the weathering product of pyrite (Garvie 1999). It changes into ferrinatrite, $Na_3Fe(SO_4)_3\cdot 3H_2O$, by contact with sulfuric acid and into metasideronatrite $Na_2Fe(SO_4)_2(OH)\cdot H_2O$ by partial dehydration (Palache et al. 1951). For these reasons, it is one of the environmental indicators of soil-water processes operating in specific landscapes, and, as such, an important marker of acid mine drainage pollution. Césbron (1964) investigated a sideronatrite specimen from Sierra Gorda (Chile) as part of a general study dealing with sulfate minerals discovered in the Chilean desert areas. This author determined, by means of X-ray rotation photographs the lattice parameters [a = 7.27(2), b = 20.50(3), c = 7.15(2) Å] and assigned, on the basis of systematic absences, the space group *Pbnm*. Moreover, from the results of thermogravimetric analysis, Césbron (1964) deduced that the three water molecules present in the compound have different structural roles. Scordari (1981a) stated, on the basis of a careful analysis of the diffraction patterns, that the structure of sideronatrite is not fully ordered and should be classified as an OD structure. Additionally, this author argued, from crystallographic, chemical, and physical considerations, that the structure should be based on ferric-sulfate chains of 7 Å periodicity.

The extensive disorder displayed has hampered to date a complete structural determination of this mineral. Fortunately during new systematic investigations via single-crystal X-ray diffraction, we found a crystal showing only a few weak diffuse streaks in the diffraction pattern, thus being suitable for a complete structural study.

The present paper gives a detailed description of the solved and refined crystal structure of the orthorhombic polytype of sideronatrite, and, on the basis of the structural model obtained, a complete description of its OD character.

EXPERIMENTAL AND STRUCTURE DETERMINATION

The crystals examined in this study were hand picked from a sample originating from Sierra Gorda (Chile). Sideronatrite forms minute needles elongated on [001], having vitreous luster and lemon-yellow color. The mineral exhibits good {010} and imperfect {100} cleavage and is associated with jarosite. Quantitative

* E-mail: f.scordari@geomin.uniba.it

electron microprobe analysis (EPMA) data were obtained with a CAMECA SX-50 electron microprobe at the Istituto di Geologia Ambientale e Geoingegneria (IGAG), CNR, Rome, operating in full wavelength dispersive (WDS) mode. The working conditions were 15 kV accelerating voltage, 15 nA beam current, 15 s peak counting times, and 10 μm beam size. The average of the microprobe analyses (Table 1) carried out on ~20 spots using two crystals confirmed a chemical composition close to the ideal formula. Chemical analysis of the associated jarosite is also reported in Table 1.

Several crystals (~40) were mounted on a Bruker AXS X8 APEX II automated diffractometer (Bruker 2003), equipped with a CCD detector, with the [001] direction parallel to the phi-axis of the four-circle Kappa goniometer, and examined with graphite-monochromatized Mo$K\alpha$ X-radiation. A single crystal, which showed minor effects of diffuse streaks in the preliminary acquisition of diffraction frames, was selected for the structural study. The intensity data were accurately recorded by a combination of several ω and φ rotation sets with 0.5° scan width. The package SAINT-IRIX (Bruker 2001) was used for data reduction, including intensity integration; moreover the data were corrected for Lorentz, polarization, background effects, and scale variation. The final unit-cell parameters were obtained from the *xyz* centroids of the measured reflections after integration. A semi-empirical absorption correction (Blessing 1995) based on the determination of transmission factors for equivalent reflections was applied by means of the SADABS software (Sheldrick 2004). Experimental details and some crystallographic data are given in Table 2.

TABLE 1. Chemical composition (wt%) for: sideronatrite [1 = from Sierra Gorda (Césbron 1964); 2 = from Antofagasta (Césbron 1964); 3 = this study]; jarosite (4) associated with the sample at hand

	1	2	3	4
SO_3	42.98	43.38	43.11(71)	31.69(53)
P_2O_5	–	–	0.011(5)	0.078(5)
SiO_2	–	–	0.048(12)	0.016(9)
Al_2O_3	–	–	0.017(5)	0.049(5)
Fe_2O_3	22.40	22.54	21.47(59)	46.95(61)
TiO_2	–	–	0.015(5)	0.239(5)
MgO	–	–	0.017(6)	0.022(9)
MnO	–	–	0.014(4)	0.012(6)
CaO	–	–	0.014(6)	0.007(4)
Na_2O	17.00	16.40	16.20(56)	0.96(6)
K_2O	–	–	0.037(16)	7.83 (16)
Cl	–	–	0.006(4)	0.004(3)
H_2O	17.75	17.96	n.d.	n.d.
Total	100.13	100.28	80.959	87.857

TABLE 2. Size, refined cell parameters, data-collection parameters, and structure refinements details

Crystal dimensions (mm)	0.160 × 0.060 × 0.020
Unit-cell dimensions	
a (Å)	7.265(2)
b (Å)	20.522(6)
c (Å)	7.120(2)
Volume (Å^3)	1061.5(5)
Z	4
Space group	$P2_12_12_1$
X-ray radiation/power	Mo$K\alpha$ (l = 0.71073 Å)/50 kV, 30 mA
Temperature (K)	298
Frame number/width/time	700/0.5°/30 s
θ range for data collection (°)	4–36.3
Index range	$-11 \le h \le 12$, $-34 \le k \le 32$, $-11 \le l \le 3$
Reflections collected/ unique/*R* merging [R_{int}]* (%)	10602/2888/7.21
Reflections used	798 with $I > 3\sigma(I)$
Completeness to θ = 36.3	99.8
Redundancy	3.12
No. of refined parameters	58
R_1† (on *F*)/wR_2‡ (on F^2)	0.0736/0.0802
$(\Delta/\sigma)_{max}$	0.00167
Goof§	1.356
$\Delta\rho_{min}/\Delta\rho_{max}$(e/Å^3)	–0.961/+0.848

* $R_{int} = \Sigma|F_o^2 - F_o^2(\text{mean})|/\Sigma[F_o^2]$.
† $R_1 = \Sigma[|F_o| - |F_c|]/\Sigma|F_o|$.
‡ $wR_2 = \{\Sigma[w(F_o^2 - F_c^2)^2]/\Sigma[w(F_o^2)^2]\}^{1/2}$.
§ Goodness-of-fit $S = \{\Sigma[w(F_o^2 - F_c^2)^2]/(n-p)\}^{0.5}$, *n* is the number of reflections and *p* is the total number of parameters refined.

Statistical analysis of the normalized structure factor distribution performed by the XPREP software utility (Sheldrick 2003), indicated the space group to be $P2_12_12_1$. The crystal structure was solved by direct methods using the SIR2004 package (Burla et al. 2005). The resulting *E*-map revealed a satisfactory correct structural model with all 17 independent atomic positions (excluding hydrogen atoms).

The least-squares refinements were carried out using the program CRYSTALS (Betteridge et al. 2003). Scattering curves for neutral chemical species were used and only reflections with $I > 3\sigma(I)$ were considered suitable for the structure refinement. Because of the OD character of the structure, the Ďurovič effect (Nespolo and Ferraris 2001) was taken into account. Therefore the reflections used in refinement [indexed with respect to the unit cell $a = 7.265(2)$, $b = 20.522(6)$, $c = 7.120(2)$ Å] were split in the following way: the reflections *hkl* with $l = 2n$, which correspond to the "family reflections" according to the OD theory, were placed into a first batch; the other reflections, namely those with $l = 2n + 1$, were placed in a second batch. The analysis was performed by refining different scales for the two batches of reflections. Refined parameters were scale factors, atomic positions, and isotropic atomic displacement parameters. The refinement was carried out taking into account a pseudo-mirror plane crossing the Fe-O-S chains, so appropriate constraints were used both for isotropic atomic displacement parameters and *x*, *y* coordinates. Finally, the introduction of anisotropic atomic displacement parameters only for Fe and S atoms led to $R = 7.4$ and $R_W = 8.0\%$. Accordingly in Table 3, the results of the refinement for all but H atoms are given. Selected bond distances and angles are reported in Table 4. A CIF[1] is on deposit. Figures 1 to 5 were drawn with the program Diamond 2.1 by Crystal Impact.

DESCRIPTION OF THE STRUCTURE

A complete and general view of the sideronatrite orthorhombic polytype structure is shown along the **a** axis in Figure l. The main feature of the crystal structure consists of Fe-octahedra, linked by *trans* (OH) vertices, to form chains parallel to the **c** axis. Two non-equivalent sulfate tetrahedra, attached by corners on alternate sides of the Fe-octahedral chain, provide further intra-chain linkages to form a structural building unit with $[Fe^{3+}(SO_4)_2(OH)]^{2-}$ composition and ~7 Å repeat distance. The Na atoms lie on two non-equivalent sites, Na1 and Na2. Each Na atom links four oxygen atoms and two water molecules forming distorted octahedra connected to each other by shared edges to form columns along the **c** axis. These edges involve, alternatively, O1 and O8 on one side, and O7 and the Ow2 on the other (Fig. 2). The Na atoms reside closer to the edge O1, O8 (O1-O8 = 3.01 Å, Na1-Na2 = 3.51 Å) than to the edge O7, Ow2 (O7-Ow2 = 3.26 Å, Na1-Na2 = 3.61 Å). These Na-columns provide the linkage among the $[Fe^{3+}(SO_4)_2(OH)]^{2-}$ chains to build infinite corrugated sheets parallel to (010). Adjacent layers are cross-linked only through hydrogen bonds, accounting for the observed perfect {010} cleavage.

The $[FeO_4(OH)_2]$ polyhedron is a nearly regular octahedron, with average bond distance of 1.999(7) Å. The individual distances involving OH are shorter [average value 1.967(5) Å] than those to O3, O4, O5, and O6 [average value 2.016(7) Å]. The two crystallographically independent tetrahedra, $[S1O_4]^{2-}$ and $[S2O_4]^{2-}$, have the typical variation in S-O bond lengths [from 1.45(1) to 1.53(1) Å]. There are slight discrepancies in the individual S-O distances. In particular, O2 is the only unshared sulfate O atom. However, it does not form the shortest distance with S as expected. However, this inconsistency is apparent because O2 takes part in a complicated hydrogen bonding system that enhances significantly its valence sum, as shown in the hydrogen bonding section. Both Na-polyhedra exhibit, within experimental error, the same mean Na-O distances (Table 4) and very similar distortions, as proved by the similar values of the quadratic elongation (λ_{Na1} = 1.00131, λ_{Na2} = 1.000691) and the bond angle variance (σ_{Na1} = 13.60, σ_{Na2} = 13.74) (Robinson et al. 1971).

Hawthorne et al. (2000), in their presentation of the structural hierarchy of sulfate minerals, placed sideronatrite among the structures with infinite chains. According to Hawthorne (1983), the sideronatrite structure can be thought of as a derivative of the tancoite, $LiNa_2H[Al(PO_4)_2(OH)]$, *Acmm* subcell. The sideronatrite structure is based on the $[M(TO_4)_2\phi]$ chain (type VI of the classification of Moore 1970). This chain is

[1] Deposit item AM-09-054, CIF. Deposit items are available two ways: For a paper copy contact the Business Office of the Mineralogical Society of America (see inside front cover of recent issue) for price information. For an electronic copy visit the MSA web site at http://www.minsocam.org, go to the American Mineralogist Contents, find the table of contents for the specific volume/issue wanted, and then click on the deposit link there.

TABLE 3. Atomic coordinates and isotropic atomic displacements parameters (Å^2) for sideronatrite, orthorhombic polytype (anisotropic atomic displacement parameters are given only for Fe and S atoms)

Atom	*x/a*	*y/b*	*z/c*	$U_{iso/eqiv}$	U_{11}	U_{22}	U_{33}	U_{23}	U_{13}	U_{12}
Fe	0.2500	0.0000	0.1250	0.0100(6)	0.0086(6)	0.0163(7)	0.0050(6)	0.0014(18)	0.0024(14)	0.0009(8)
S1	0.2251(5)	0.1317(2)	0.8781(3)	0.0139(1)	0.0070(10)	0.0252(15)	0.0096(10)	0.003(3)	–0.006(3)	0.0001(10)
S2	0.8763(4)	0.0056(2)	0.3781(3)	0.0119(1)	0.0075(10)	0.0204(15)	0.0083(10)	0.000(3)	–0.001(3)	–0.0001(10)
Na1	0.8294(6)	0.1224(2)	0.120(3)	0.0267(10)	–	–	–	–	–	–
Na2	0.8294(6)	0.1224(2)	0.627(3)	0.0267(10)	–	–	–	–	–	–
O1	0.0291(19)	0.1452(7)	0.8781(3)	0.024(3)	–	–	–	–	–	–
O2	0.3299(18)	0.1927(6)	0.8781(3)	0.025(3)	–	–	–	–	–	–
O3	0.2795(11)	0.0944(4)	0.0462(9)	0.0195(17)	–	–	–	–	–	–
O4	0.2795(11)	0.0945(4)	0.7053(9)	0.0195(17)	–	–	–	–	–	–
O5	0.9900(11)	0.0184(4)	0.5497(9)	0.0164(15)	–	–	–	–	–	–
O6	0.9900(11)	0.0184(4)	0.2019(9)	0.0164(15)	–	–	–	–	–	–
O7	0.7222(18)	0.0511(6)	0.3781(3)	0.017(3)	–	–	–	–	–	–
O8	0.687(2)	0.0625(7)	0.8781(3)	0.023(3)	–	–	–	–	–	–
OH	0.3430(15)	0.0241(5)	0.3781(3)	0.015(2)	–	–	–	–	–	–
Ow1	0.5984(16)	0.1984(5)	0.5835(17)	0.047(3)	–	–	–	–	–	–
Ow2	0.032(2)	0.1661(8)	0.3781(3)	0.035(4)	–	–	–	–	–	–
Ow3	0.5984(16)	0.1984(5)	0.1676(17)	0.047(3)	–	–	–	–	–	–

TABLE 4. Selected bond distances (Å) and angles (°) for sideronatrite orthorhombic polytype

Fe-OH	1.987(5)	S1-O1	1.451(14)	S2-O5	1.499(7)	Na1-O1‖	2.303(17)	Na2-O1**	2.349(17)
Fe-OH*	1.947(5)	S1-O2	1.467(14)	S2-O6	1.526(7)	Na1-O6	2.499(10)	Na2-O5	2.493(10)
Fe-O3	2.029(7)	S1-O3§	1.475(7)	S2-O7	1.456(14)	Na1-O7	2.472(16)	Na2-O7	2.427(16)
Fe-O4*	2.032(7)	S1-O4	1.501(7)	S2-O8†	1.471(15)	Na1-O8#	2.359(17)	Na2-O8	2.404(17)
Fe-O5†	1.999(7)	<S1-O>	1.474	<S2-O>	1.488	Na1-Ow2**	2.515(18)	Na2-Ow1	2.313(13)
Fe-O6‡	2.002(7)					Na1-Ow3	2.316(13)	Na2-Ow2**	2.471(17)
<Fe-O>	1.999					<Na1-O>	2.411	<Na2-O>	2.410
O3-Fe-OH	88.7(4)	O1-S1-O2	110.2(8)	O5-S2-O6	109.9(5)	O1‖-Na1-Ow3	115.3(7)	O1**-Na2-Ow1	114.5(6)
O3-Fe-O5†	90.4(3)	O1-S1-O3§	111.3(4)	O5-S2-O7	108.2(4)	O1‖-Na1-Ow2**	95.9(4)	O1**-Na2-Ow2**	96.1(4)
O3-Fe-O6‡	89.7(3)	O1-S1-O4	110.9(4)	O5-S2-O8†	109.8(4)	O8#-Na1-O6	86.0(4)	O8-Na2-O5	85.9(4)
O3-Fe-OH*	91.7(4)	O2-S1-O3§	107.7(4)	O6-S2-O7	107.8(4)	O8#-Na1-Ow3	98.0(6)	O8-Na2-Ow1	97.6(6)
O4*-Fe-OH*	88.6(4)	O2-S1-O4	107.3(4)	O6-S2-O8†	109.4(4)	Ow2**-Na1-Ow3	94.3(7)	Ow2**-Na2-Ow1	95.4(7)
O4*-Fe-O5†	89.7(3)	O3§-S1-O4	109.3(6)	O7-S2-O8†	111.6(8)	Ow2**-Na1-O6	81.9(6)	Ow2**-Na2-O5	82.7(5)
O4*-Fe-O6‡	90.2(3)					Ow3-Na1-O7	93.6(6)	O1**-Na2-O5	92.9(5)
O4*-Fe-OH	91.1(4)					Ow2**-Na1-O7	81.8(7)	O1**-Na2-O8	78.6(7)
O5†-Fe-OH	88.2(4)					O1‖-Na1-O8#	80.5(7)	O8-Na2-O7	95.5(3)
O5†-Fe-OH*	92.1(4)					O1‖-Na1-O6	93.1(5)	O7-Na2-Ow1	94.4(6)
O6‡-Fe-OH*	88.2(4)					O8#-Na1-O7	95.5(3)	O7-Na2-Ow2**	83.4(6)
O6‡-Fe-OH	91.5(4)					O6-Na1-O7	58.0(4)	O7-Na2-O5	58.2(4)
O3-Fe-O4*	179.7(3)					O1‖-Na1-O7	151.1(5)	O5-Na2-Ow1	152.6(7)
OH-Fe-OH*	179.46(5)					Ow3-Na1-O6	151.6(8)	O1**-Na2-O7	151.0(5)
O6‡-Fe-O5†	179.7(3)					Ow2**-Na1-O8#	167.4(5)	O8-Na2-Ow2**	167.2(6)

Notes: Symmetry code for equivalent positions: * = 0.5 – *x*, –*y*, *z* – 0.5; † = 1.5 – *x*, –*y*, *z* – 0.5; ‡ = *x* – 1, *y*, *z*; § = *x*, *y*, 1 + *z*; ‖ = 1 + *x*, y, *z* – 1; # = *x*, *y*, *z* – 1; ** = 1 + *x*, *y*, *z*.

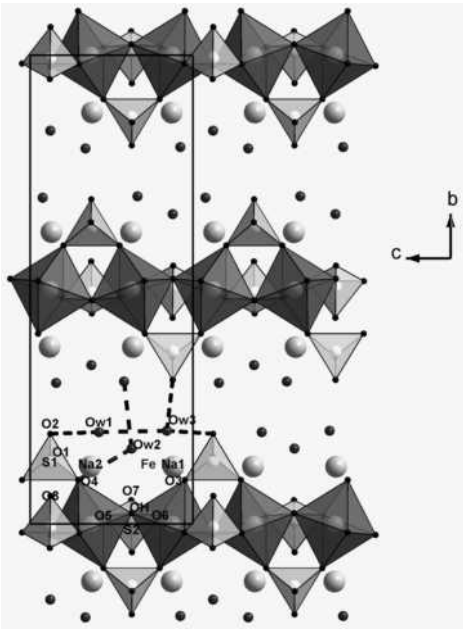

FIGURE 1. The crystal structure of sideronatrite seen along the **a** axis. The unit cell and the proposed hydrogen-bond system in sideronatrite are outlined.

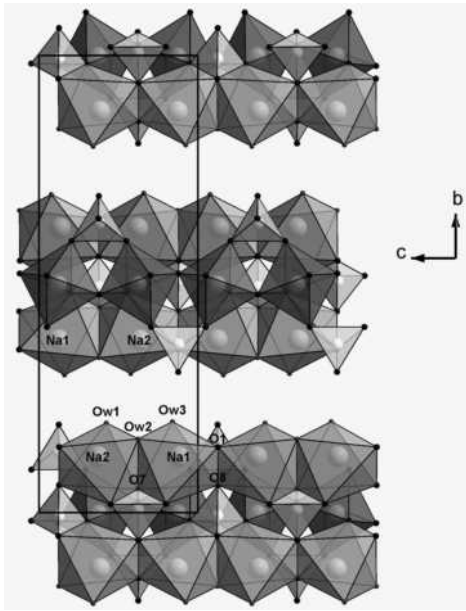

FIGURE 2. Corrugated layers present in sideronatrite showing the edge-sharing (O1-O8, O7-Ow2) between Na polyhedra and the relationships between Na-columns and Fe-S chains.

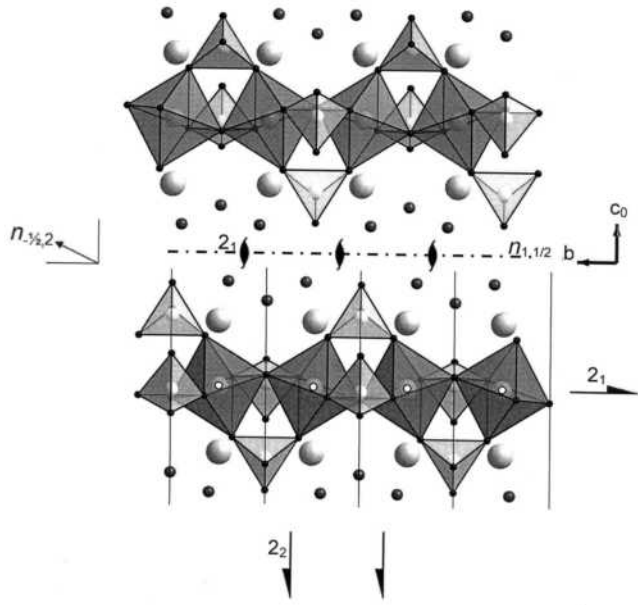

FIGURE 3. Representation of a pair of adjacent layers. The partial symmetry operations (λ- and σ-POs), as seen along the **a** axis, are indicated. The orientation of single building layer (space group symmetry $P2_1/m$) is outlined.

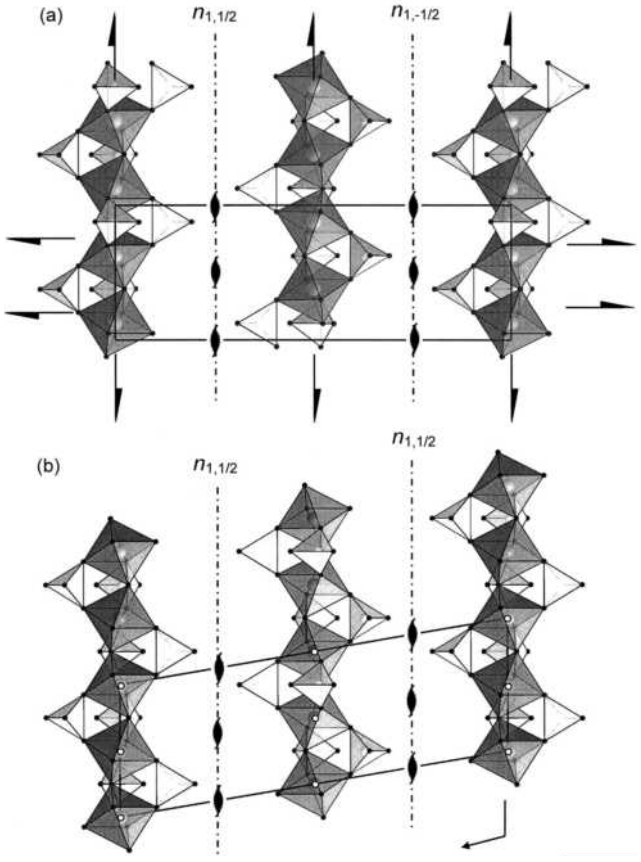

FIGURE 4. Schematic representation of MDO1 (**a**) and MDO2 (**b**) polytypes. For the sake of clarity, only Fe-O-S chains are illustrated. The sequence of $n_{1,1/2}$ σ-POs, the total symmetry operations, and the unit cells are represented in both polytypes.

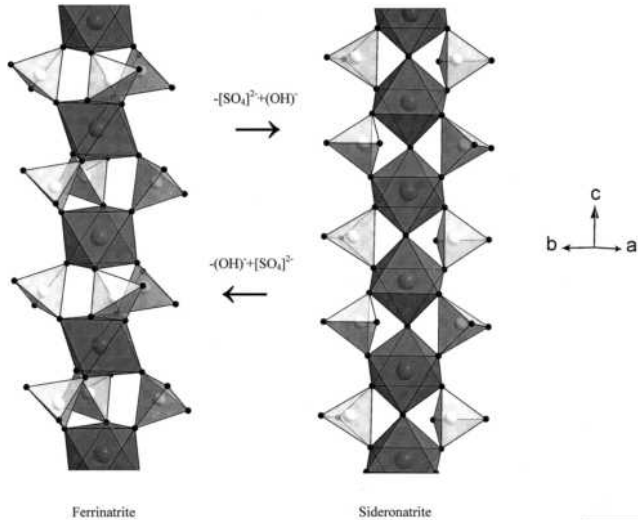

FIGURE 5. Sketch illustrating the structural rearrangement of Fe-O-S chain, connected to the basicity/acidity of the solution during the reversible phase transition ferrinatrite ↔ sideronatrite.

also present in other sulfate phases, for example guildite, $CuFe(SO_4)_2(OH)\cdot 4H_2O$, (Wan et al. 1978), whereas it is topologically identical to the one found in transition metal phosphates like tancoite, $LiNa_2H[Al(PO_4)_2(OH)]$, (Hawthorne 1983), jahnsite, $[CaMnFe_2^{3+}(PO_4)_4(OH)_2][Mg(H_2O)_4]_2$, (Moore and Araki 1974) overite, $[Ca_2Al_2(PO_4)_4(OH)_2][Mg(H_2O)_4]_2$ (Moore and Araki 1977), and segelerite, $[Ca_2Fe_2^{3+}(PO_4)_4(OH)_2][Mg(H_2O)_4]_2$ (Moore and Araki 1977). The main difference between sideronatrite and guildite is in the different types of sheet structure, with the $[Fe^{3+}(SO_4)_2(OH)]^{2-}$ chains in guildite cross-linked through isolated $[CuO_2(H_2O)_4]$ octahedra.

HYDROGEN BONDING

Owing to the imperfect quality of the reflections with $l = 2n + 1$, the system of hydrogen bonds could not be derived directly by difference-Fourier synthesis. A possible hydrogen bonding scheme was deduced by cross-checking electrostatic bond valence requirements and geometric considerations. The data of Breese and O'Keeffe (1991) were used to calculate the electrostatic bond strengths of all the non-H atoms (Table 5).

The valence sums of the bond strengths reaching each oxygen ($\Sigma_c v$), reported in Table 5, confirm that the OH atom shared between two consecutive Fe atoms belongs to a hydroxyl group, whereas Ow1, Ow2, and Ow3 belong to water molecules. From the inspection of Table 5, we note that O2, O4, and O7 show apparent electrostatic undersaturation, so these O atoms are expected to have the function of proton acceptors in the system of hydrogen bonds.

From the analysis of the possible neighbor acceptors around the hydroxyl group, it is apparent that the hydrogen interacts with O7, shared by S2, Na1, and Na2. The combined analysis of the suitable interatomic O-O distances and angles between the water molecule and the undersaturated O atoms leads to a reliable hydrogen bonding system illustrated in Figure 1. As a matter of fact, the bond valence sums for the scheme obtained through geometric considerations, and computed considering the hydrogen bond contributions on the basis of the O-O distances (Ferraris and Ivaldi 1988), appear quite satisfactory (Tables 5–6).

TABLE 5. Bond valence balance for sideronatrite calculated according to Breese and O'Keeffe (1991) and Ferraris and Ivaldi (1988)

Atom	O1	O2	O3	O4	O5	O6	O7	O8	OH	Ow1	Ow2	Ow3	$\Sigma_a V$
Fe			0.482	0.478	0.523	0.519			{ 0.602 0.540				3.144
S1	1.596	1.529	1.496	1.394									6.015
S2					1.402	1.303	1.575	1.512					5.792
Na1	0.259					0.152	0.164	0.223			0.146	0.250	1.194
Na2	0.229				0.155		0.185	0.197		0.252	0.164		1.182
$\Sigma_c V$	2.084	1.529	1.978	1.872	2.080	1.974	1.924	1.932	1.142	0.252	0.310	0.250	
$\Sigma'_c V$	2.084	2.039	1.978	1.965	2.080	1.974	2.104	1.932	1.962	2.123	2.046	2.040	

Note: $\Sigma_c V$ is the sum of bond strengths reaching the anions; $\Sigma'_c V$ after correction for hydrogen bonds.

TABLE 6. O···O distances (Å), hydrogen bonding angles, and hydrogen bond strengths (v.u.)

	O···O (Å)	v.u.		O···Ow···O(°)
Ow1-Ow3	2.961	0.138	O2†-Ow3-O2*	111.0
Ow1-O2	2.866	0.162	O2-Ow1-Ow3	137.0
Ow2-O4	3.291	0.093	O4-Ow2-Ow1	106.1
Ow2-Ow1*	2.836	0.171		
Ow3-O2*	2.815	0.178		
Ow3-O2†	2.840	0.170		
OH-O7	2.810	0.180		

Notes: In each pair of hydrogen bonded oxygen atoms, the first oxygen is the donor, the second one is the acceptor. Hydrogen bond strengths were calculated according Ferraris and Ivaldi (1988). Atom at:
* = ½ + *x*, ½ – *y*, 1 – *z*;
† = *x*, *y*, *z* – 1.

OD CHARACTER ANALYSIS

Scordari (1981a), from the coexistence in the diffraction pattern of sharp spots for l = 2n and diffuse streaks (elongated Bragg reflections) parallel to **b*** for l = 2n + 1, found that sideronatrite crystals are commonly disordered along the **b** axis, and interpreted this as due to the OD nature of the structure. The success of the structure solution allows us to give a description of the sideronatrite structure in terms of OD theory. Sideronatrite belongs to a family of OD structures formed of equivalent layers of $Na_2Fe(SO_4)_2(OH)\cdot 3H_2O$ composition. The symmetry properties of the whole family are encompassed by an appropriate individual OD groupoid family symbol (see Ferraris et al. 2004 for a complete review of the OD theory). This notation consists of two lines. The first line of the symbol gives the symmetry operations that bring each single layer into itself (λ-operations) and thus the plane group of the single layer. The second line gives the set of symmetry operations relating adjacent layers (σ-operations). These operations are called partial operations (POs) in OD theory because they are not necessarily valid for the whole structure. The symbols for these operators conform to the ones used in normal space group operations.

To describe all the possible structures of sideronatrite by the standard OD groupoid family symbol, consistent with that in the basic compilation of Dornberger-Schiff and Fichtner (1972), the **b** and **c** axes of the single layer must be interchanged with respect to those so far assumed in the crystal-structure description of sideronatrite. Henceforth, in this paper, the transformed unit cell will be maintained in the development of the OD approach. Accordingly, the basic OD layer crystallographic parameters are: a = 7.265 and b = 7.120, width c_0 = 10.261 Å, where c_0 is one half of the b translation in the orthorhombic polytype cell, and symmetry defined by the layer group $P2_1/m$ (see Fig. 3).

The OD-groupoid symbol is the following:

$$P\ 1 \quad 2_1/m \quad (1)$$
$$\{2_r/n_{s-1,2} \quad 1 \quad (2_2/n_{r,s})\}$$

The parentheses at the last place of each line indicate the direction of missing periodicity. The r and s indices that characterize the σ-translations in the second line assume, in the present case, the following values: r = 1 and s = 1/2. Sideronatrite is a category I (Ferraris et al. 2004) OD structure presenting λ- and σ-POs with τ and ρ character. A τ-PO leaves the layer upside up, whereas the ρ-PO turns the layer upside down. For the presence of the mirror plane in the single building layer, adjacent layers can be stacked in an equivalent way either by the operation $n_{1,+1/2}$ (glide plane normal to the **c** axis and with translation component **a**/2+**b**/4) or by the operation $n_{1,-1/2}$ (glide plane normal to the **c** axis and with translation component **a**/2–**b**/4). The same considerations hold for the operation $n_{\pm 1/2,2}$ (glide plane normal to the **a** axis and with translation component $\mathbf{c_0}\pm\mathbf{b}/4$). Pairs of layers related by either of the two operations are geometrically equivalent. An infinite number of different polytypes, depending on the stacking sequence, may exist: all these polytypes form an OD family. The symmetry of each possible polytype can be derived from the symmetry properties of the family embodied in the OD-groupoid family symbol. Among all possible ordered stacking sequences, there are two in which not only couples, but also triples (quadruples...n-ples) of adjacent layers are geometrically equivalent. These are the so-called maximum degree order (MDO) structures. For sideronatrite, we have only two possible MDO polytypes: (1) if $n_{-1/2,2}$ $n_{+1/2,2}$ σ-operators regularly alternate, the first and third layer are simply $2\mathbf{c_0}$ translated, so the 2_2 σ-operator is continued through the entire sequence of layers, becoming a 2_1 total symmetry operator in the structure with $\mathbf{c} = 2\mathbf{c_0}$. Besides, the 2_1 σ-operator is constantly repeated by $\mathbf{c_0}$, acting as a total symmetry element. Therefore the space group of the resulting MDO1 polytype is $P2_12_12_1$ with cell parameters a = 7.265, b = 7.120, and c = 20.522 Å (Fig. 4a), corresponding to the above described structure in all but the orientation of the axes, with the 7 Å ferric-sulfate chains parallel to the z axis in line with other similar structures; (2) if the $n_{-1/2,2}$ σ-operator is constantly applied, the first and third layer are now translated by the vector $\mathbf{b}/2+2\mathbf{c_0}$. The $n_{-1/2,2}$ σ-operator becomes a glide plane valid for the whole structure with $\mathbf{c} = \mathbf{b}/2+2\mathbf{c_0}$. The 2_1 σ-operator, is now translated by the translational vector, and is valid for this MDO2 polytype, with monoclinic symmetry, space group $P2_1/c$, and lattice parameters a = 7.265, b = 7.120, c = 20.828 Å, and α = 99.84° (Fig. 4b). Transformed to a standard setting with the 7 Å ferric-sulfate chains parallel to the z axis, the MDO2 polytype has space group $P2_1/a$ and cell parameters a = 20.828, b = 7.265, c = 7.120 Å, and β = 99.84°. Of course the opposite regular stacking

sequence gives rise to a twin related polytype.

According to the Ramsdell symbol (Verma and Krishna 1966), the MDO1 and MDO2 polytypes should be denoted as sideronatrite-2*O* and sideronatrite-2*M*, respectively. The ideal symmetry of the single layer is not maintained in the real structure of the MDO1 polytype, which actually presents a desymmetrization (i.e., losing of inversion axis); on the contrary, it is preserved in the possible real structure of the MDO2 polytype. Therefore a hypothetical structural model for the polytype MDO2 was suggested, starting from the atomic positions of the single layer present in the MDO1 polytype and adding the inversion axis. Calculated atomic coordinates are given in Table 7.

All disordered and ordered structures of the same OD family display diffraction patterns with common reflections, "family reflections." These reflections are always sharp and have the same positions and intensities in all the OD structures of the family not depending on the degree of disorder in the stacking sequence. The family reflections arise from a fictitious structure, periodic in three dimensions, closely related to the real structures of the family members and called "family structure" or "superposition structure." The distribution of these sharp reflections, in reciprocal space, is deducible from the analysis of the Fourier transform of the whole structure. Following the procedures described by Merlino (1997), the Fourier transform of the entire structure can be obtained by summing the contributions of the all layers, taking into account their relative positions. In the case at hand, adjacent layers can be related by the $n_{1,\pm1/2}$ operator (or by $n_{\pm1/2,2}$). Therefore, if we indicate $\phi_0(hk\zeta)$ as the contribution of the layer L_0, the next layer, L_1, gives a contribution: $\phi_1(hk\zeta) = \phi_0(\bar{h}k\zeta)$ $\exp[2\pi i(h/2 \pm k/4 + \zeta)]$, owing to every atom at x_i, y_i, z_i in the layer L_0, there is an equivalent atom at $-x_i+1/2$, $y_i \pm 1/4$, $z_i + 1$ in the layer L_1. The indices h and k are integer numbers, whereas ζ may be arbitrary. In any stacking sequence of an ordered or disordered structure, all even layers L_{2p} and all odd layers L_{2p+1} are translationally equivalent to the zero layer, L_0, and the first layer, L_1, respectively, through the vector: $T_{2p} = \alpha\mathbf{b}/2 + 2p\mathbf{c_0}$, with $\alpha = 0, \pm1$, corresponding to the two possible stacking combinations, and p being an integer. The total Fourier transform, summing the contributions of both even and odd layers, is:

$$F(hk\zeta) = [\phi_0(hk\zeta) + \phi_1(hk\zeta)]$$

$$\frac{1}{2M}\sum \exp\left[2\pi i\left(\alpha\frac{k}{2} + 2p\zeta\right)\right] = [\phi_0(hk\zeta) + \phi_1(hk\zeta)]\ S(hk\zeta)$$

If k = 2K, the expression of $S(hk\zeta)$ is independent of the parameter α and, therefore, of the degree of disorder. With a large number M of layers, $S(hk\zeta)$ vanishes except for $\zeta = 1 = L/2$. Therefore the diffraction pattern of any member in the OD family will show sharp reflections with even k (family reflections). These family reflections correspond to a reciprocal lattice with lattice vectors **A*** **B*** and **C*** that are related to the basic vectors **a*** **b*** **c*** as follows: **A*** = **a***, **B*** = **b***/2 and **C*** = 2**c***/2. So the fictitious superposition structure is closely related to the structures of the family and displays, in the present case, space group *Pnmn* with lattice constants a = 7.265, b = 3.56, c = 20.562 Å.

TABLE 7. Calculated atomic coordinates for monoclinic polytype (MDO2)

Atom	*x/a*	*y/b*	*z/c*
Fe1	0.0000	0.0000	0.0000
Fe2	0.0000	0.0000	0.5000
S1	0.1319	–0.0260	0.8160
S2	0.0066	0.6259	0.2533
Na1	0.1224	0.5800	0.0562
Na2	0.1224	0.5800	0.5662
O1	0.1434	–0.2300	0.8217
O2	0.1925	0.0810	0.8463
O3	0.0940	0.0280	–0.0280
O4	0.0940	0.0280	0.6220
O5	0.0180	0.7420	0.4340
O6	0.0180	0.7420	0.0840
O7	0.0510	0.4670	0.2755
O8	0.0600	0.4510	0.7800
OH	0.0230	0.0910	0.2645
Ow1	0.1970	0.3450	0.5535
Ow2	0.1610	–0.2080	0.3305
Ow3	0.1970	0.3450	0.1435

Note: Space group $P2_1/a$; cell parameters: a = 20.828, b = 7.265, c = 7.120 Å, β = 99.84°.

Chemical and structural relations of sideronatrite with paragenetic minerals

As stated above, sideronatrite is associated with other secondary sulfates (Palache et al. 1951) and in particular with ferrinatrite, $Na_3[Fe(SO_4)_3]\cdot 3H_2O$, at the Mina de la Compania, near Sierra Gorda (Chile), and with voltaite, $K_2[Fe^{2+}_5Fe^{3+}_3Al(SO_4)_{12}]\cdot 18H_2O$, at Potosi (Bolivia). In addition, it has been observed that ferrinatrite occurs at Chuquicamata with metasideronatrite, $Na_2Fe(SO_4)_2(OH)\cdot 2H_2O$, and with metavoltine, $K_2Na_6(Fe^{2+},Zn)[Fe^{3+}_6O_2(SO_4)_{12}]\cdot 18H_2O$ (Palache et al. 1951).

Actually, metasideronatrite can be produced from sideronatrite by dehydration over sulfuric acid (Palache et al. 1951), or more simply at ambient temperature changing the humidity (Garvie 1999). Finally metasideronatrite can be converted into ferrinatrite by treatment of this mineral with a solution of sodium sulfate and sulfuric acid (Palache et al. 1951).

Several papers deal with the question of solid-state reactions and, more in general, with that of the phase transitions in these kind of compounds (Scordari 1980a, 1980b, 1981a, 1981b, 1983; Scordari and Stasi 1990; Scordari et al. 1994a, 1994b). The reader is referred to them to get a deeper knowledge on this matter. In short, here we consider the chemical and structural relationships and the paragenetic sequence that could explain the voltaite, ferrinatrite, sideronatrite, and metasideronatrite association.

Let us first consider polyhedra populated by higher-bond-valence cations, which form the fundamental building block (FBB) according to Hawthorne (1985). Voltaite (Mereiter 1972) could be the first mineral to crystallize starting from a solution rich in H_2SO_4. In fact, in voltaite, with $Fe^{3+}/(SO_4)^{2-} = 1/4$, the large uptake of $(SO_4)^{2-}$ groups in the structure prevent the Fe-O-S chain formation observed in ferrinatrite and sideronatrite. Consequently ^{XII}K-polyhedra and $Fe(O,H_2O)$-octahedra are linked by $(SO_4)^{2-}$ tetrahedra to form a framework of cages, inside of which $Al(H_2O)_6$ octahedra are located. Ferrinatrite, with $Fe^{3+}/(SO_4)^{2-} = 1/3$ [i.e., the minimum value the ratio can assume for the polymerization of Fe-octahedra and $(SO_4)^{2-}$ tetrahedra into chains], very likely crystallizes after voltaite. Last, in the crystallization sequence there is sideronatrite, which has the higher ratio $Fe^{3+}/(SO_4)^{2-} = 1/2$. Metasideronatrite can be derived from

sideronatrite simply by dehydration. The solid-state reaction is easy and reversible and involves the presence/absence of two water molecules coordinated by Na atoms that affect only the topology of Na-O columns.

According to the structural formulae shown above, in ferrinatrite $[Fe^{3+}(SO_4)_3^{2-}]^{3-}$, clusters polymerize to form chains running along the **c** axis. The same occurs in sideronatrite in which clusters of composition, $[Fe^{3+}(SO_4)_2^{2-}OH]^{2-}$, polymerize to originate chains that develop also in the **c** direction. Following Palache et al. (1951), sideronatrite can be transformed into ferrinatrite by contact with concentrated sulfuric acid. As inferred from the formulae quoted above, the main difference between sideronatrite and ferrinatrite is one Na more to compensate the replacement of OH^- by O^{2-} owing to the entrance of an additional $(SO_4)^{2-}$ group in the latter compound.

The complete chemical reaction that describes the change sideronatrite → ferrinatrite is the following:

$$4Na_2Fe^{3+}(OH)(SO_4)_2\cdot 3H_2O + 2H_2SO_4 \rightarrow$$
(sideronatrite)
$$2Na_3Fe^{3+}(SO_4)_3\cdot 3H_2O + Fe_2^{3+}(SO_4)_3 + Na_2SO_4 + 10H_2O.$$
(ferrinatrite)

The same transformation has been observed in metasideronatrite. This mineral, as stated above, can be easily produced from sideronatrite over sulfuric acid, and if it is treated with a solution of sodium sulfate and sulfuric acid (Palache et al. 1951) undergoes the same solid-state reaction observed in sideronatrite:

$$4Na_2Fe^{3+}(OH)(SO_4)_2\cdot H_2O + 2H_2SO_4 + Na_2SO_4 \rightarrow$$
(metasideronatrite)
$$2Na_3Fe^{3+}(SO_4)_3\cdot 3H_2O + Fe_2^{3+}(SO_4)_3 + 2Na_2SO_4 + 2H_2O.$$
(ferrinatrite)

As a matter of fact, the compound Na_2SO_4 does not take part to the building of the new phase (ferrinatrite), so, as in sideronatrite, only the presence of the sulfuric acid is necessary to prime the reaction. Finally, on standing in damp air, ferrinatrite changes to sideronatrite (Palache et al. 1951), according to the chemical reaction:

$$2Na_3Fe^{3+}(SO_4)_3\cdot 3H_2O + 2H_2O \rightarrow$$
(ferrinatrite)
$$2Na_2Fe^{3+}(OH)(SO_4)_2\cdot 3H_2O + Na_2SO_4 + 2H_2SO_4$$
(sideronatrite)

From a structural point of view, the OH^- group is the corner shared by two neighboring Fe^{3+}-octahedra in sideronatrite. This OH^- group can be replaced by a $[(SO_4)]^{2-}$ group that, together with two similar groups already present in sideronatrite, works as a bridge between two neighboring Fe^{3+}-octahedra in ferrinatrite (Fig. 5). We observe that this replacement can occur if the electroneutrality of the structure is preserved, and this occurs if a monovalent cation enters the structure according to: $OH^- \rightarrow (SO_4)^{2-} + Na^+$. As observed above, the structure of sideronatrite is based on corrugated sheets of $Na_2[Fe^{3+}(OH)(SO_4)_2]\cdot 3H_2O$ composition. The entrance of the Na^+ cation [together with the $(SO_4)^{2-}$ group] into the structure of sideronatrite changes the topology of Na-columns because $Na\varphi_6$ (where φ is H_2O, O^{2-}) octahedra present in sideronatrite increase their coordination number, forming $Na\varphi_7$-polyhedra. The Na^+ cations, differently from sideronatrite, arrange themselves around chains of $[Fe^{3+}(SO_4)_3]^{3-}$ composition to form a three-dimensional network of bonds in ferrinatrite.

The sideronatrite from Sierra Gorda investigated here is associated with jarosite, $KFe_3^{3+}(OH)_6(SO_4)_2$. This mineral has the highest ratio in respect to the compounds considered above, i.e., $Fe^{3+}/(SO_4)^{2-} = 3/2$. In the jarosite structure, $Fe^{3+}(OH)_4O_2$ octahedra share four OH^- corners to form sheets, with three- and six-membered rings parallel to (001). The high Fe content compared to $(SO_4)^{2-}$ groups lets us suppose that, owing to the $(SO_4)^{2-}$ impoverishment, jarosite may be the last mineral crystallizing from a K-poor solution in the paragenetic sequence discussed here.

Acknowledgments

The authors are grateful to Marcello Serracino for assistance during electron probe microanalyses at the Istituto di Geologia Ambientale e Geoingegneria, CNR, Rome. Financial support was provided by Fondi di Ateneo 2008.

References cited

Betteridge, P.W., Carruthers, J.R., Cooper, R.I., Prout, K., and Watkin, D.J. (2003) Crystals version 12: software for guided crystal structure analysis. Journal of Applied Crystallography, 36, 1487–1492.

Blessing, R.H. (1995) An empirical correction for absorption anisotropy. Acta Crystallographica, A51, 33–38.

Breese, N.E. and O'Keeffe, M. (1991) Bond-valence parameters for solids. Acta Crystallographica, B47, 192–197.

Bruker (2001) SAINT. Bruker AXS Inc., Madison, Wisconsin.

——— (2003) APEXII. Bruker AXS Inc., Madison, Wisconsin.

Burla, M.C., Caliandro, R., Camalli, M., Carrozzini, B., Cascarano, G., De Caro, E., Giacovazzo, C., Polidori, G., and Spagna, R. (2005) SIR2004: An improved tool for crystal structure determination and refinement. Journal of Applied Crystallography, 38, 381–388.

Césbron, F. (1964) Contribution à la minéralogie des sulphates de fer hydratés. Bulletin Societe Francais de Mineralogie et Crystallographie, 87, 125–143.

Cleve, P.T. (1870) Ak. Stockholm Handl., 9, 31. Cited in Palache, C., Berman, H., and Frondel, C. (1951) The System of Mineralogy, 7th edition, vol. 2, 1124 p. Wiley, London.

Dornberger-Schiff, K. and Fichtner, K. (1972) On the symmetry of OD-structures consisting of equivalent layers. Kristall und Technik, 7, 1035–1056.

Ferraris, G. and Ivaldi, G. (1988) Bond valence *vs* bond length in O...O hydrogen bonds. Acta Crystallographica, B44, 341–344.

Ferraris, G., Makovicky, E., and Merlino, S. (2004) Crystallography of modular materials, 15, 370 p. International Union of Crystallography Monographs on Crystallography, Oxford Science Publications, U.K.

Frenzel, A. (1879) Mineralogische und petrographische Mitteilungen, 2, 133. Cited in Césbron, F. (1964) Contribution à la minéralogie des sulphates de fer hydratés. Bulletin de la Société Française ae Minéralogie et de Cristallographie, 87, 138.

Garvie, L.A.J. (1999) Sideronatrite and metasideronatrite efflorescence formed in a coastal sea-spray environment. Mineralogical Magazine, 63, 757–759.

Hawthorne, F.C. (1983) The crystal structure of tancoite. Tschermaks Mineralogische und Petrographische Mitteilungen, 31, 121–135.

——— (1985) Towards a structural classification of minerals: the $^{VI}M^{IV}T_2O_n$ minerals. American Mineralogist, 70, 455–473.

Hawthorne, F.C., Krivovichev, S.V., and Burns, P.C. (2000) The crystal chemistry of sulfate minerals. In C.N. Alpers, J.L. Jambor, and B.K. Nordstrom, Eds., Sulfate Minerals—Crystallography, Geochemistry, and Environmental Significance, 40, p. 1–112. Reviews in Mineralogy and Geochemistry, Mineralogical Society of America, Chantilly, Virginia.

Mereiter, K. (1972) Die kristallstruktur des voltaits, $K_2Fe_5^{2+}Fe_3^{3+}Al[SO_4]_{12}\cdot 18H_2O$. Tschermaks Mineralogische und Petrographische Mitteilungen, 18, 185–202.

Merlino, S. (1997) OD approach in minerals: examples and applications. In S.Merlino, Ed., Modular Aspects of Minerals, 1, p. 29–54. EMU Notes in Mineralogy, Eötvös University Press, Budapest.

Moore, P.B. (1970) Structural hierarchies among minerals containing octahedrally coordinating oxygen: I. Stereoisomerism among corner-sharing octahedral and tetrahedral chains. Neues Jahrbuch für Mineralogie, Monatshefte, 163–173.

Moore, P.B. and Araki, T. (1974) Jahnsite, $CaMn^{2+}Mg_2(H_2O)_8Fe_2^{3+}(OH)_2[PO_4]_4$: A

novel stereoisomerism of ligands about octahedral corner-chains. American Mineralogist, 59, 947–963.
——— (1977) Overite, seglerite, and jahnsite: A study in combinatorial polymorphism. American Mineralogist, 62, 692–702.
Nespolo, M. and Ferraris, G. (2001) Effects of the stacking faults on the calculated electron density of mica polytypes—The Durovic effect. European Journal of Mineralogy, 13, 1035–1045.
Palache, C., Berman, H., and Frondel, C. (1951) The System of Mineralogy, Volume II, 7th edition, p. 604–605. Wiley, New York.
Raimondi, A. (1878) Mineraux du Perou: Catalogue raisonné d'une collection des principaux types minéraux de la République, p. 233. A. Chaix et Cie, Paris.
Robinson, K., Gibbs, G.V., and Ribbe, P.H. (1971) Quadratic elongation, a quantitative measure of distortion in coordination polyhedra. Science, 172, 567–570.
Scordari, F. (1980a) Structural considerations of some natural and artificial alkali iron hydrated sulfates. Mineralogical Magazine, 43, 669–673.
——— (1980b) The structure of $K_2(K_{0.41},H_2O_{0.59})_6Na_{3.98}H_3O^+_{0.78}X^+_{0.68}(Fe^{2+}_{0.05}$, $vacancy_{0.95})Fe^{3+}_6O_2(SO_4)_{12}.11.91H_2O$: a compound related to metavoltine and α-Maus's salt. Acta Crystallographica, B36, 1733–1738.
——— (1981a) Sideronatrite: A mineral with a $Fe(SO_4)(OH)$ guildite-type chain? Tschermaks Mineralogische und Petrographische Mitteilungen, 28, 315.
——— (1981b) Crystal chemical implications on some alkali hydrated sulphates. Tschermaks Mineralogische und Petrographische Mitteilungen, 28, 207–222.
——— (1983) Solid-state reactions in "salt X." Zeitschrift für Kristallographie, 163, 31–41.
Scordari, F. and Stasi, F. (1990) Analysis of the compound $K_{3.86}Na_{5.30}H_3O^+_{0.84}Fe^{3+}_6O_2$ $(SO_4)_{12}\cdot 17.08H_2O$: Structure, crystal chemistry, and stability. Zeitschrift für Kristallographie, 190, 47–62.
Scordari, F., Stasi, F., Schingaro, E., and Comunale, G. (1994a) Analysis of the $[Na_{1/3}, (H_2O)_{2/3}]_{12}[NaFe^{3+}O(SO_4)_6(H_2O)_3]$ compound: Crystal structure, solid state transformation, and its relationship to some analogues. Zeitschrift für Kristallographie, 209, 43–48.
——— (1994b) A survey of $(Na, H_3O^+, K)_5Fe_3O(SO_4)_6\cdot nH_2O$ compounds: architectural principles and influence of the Na-K replacement on their structures. Zeitschrift für Kristallographie, 209, 733–737.
Sheldrick, G.M. (2003) XPREP. Bruker-Nonius AXS, Madison, Wisconsin.
——— (2004) SADABS, Program for empirical absorption correction of area detector data. University of Göttingen, Germany.
Van Tassel, R. (1956) Sideronatrite dans des charbonnages belfes. Bulletin: Institut Royal des Sciences Naturelles de Belgique, 32, 1–4.
Verma, A.J. and Krishna, P. (1966) Polymorphism and Polytypism in Crystals, 341 p. Wiley, New York.
Wan, C., Ghose, S., and Rossmann, G.R. (1978) Guildite, a layer with a ferric hydrous-sulfate chain and its optical absorption spectra. American Mineralogist, 63, 478–483.

MANUSCRIPT RECEIVED MAY 7, 2009
MANUSCRIPT ACCEPTED AUGUST 5, 2009
MANUSCRIPT HANDLED BY G. DIEGO GATTA